

## Coherent tunneling by adiabatic passage in an optical waveguide system

S. Longhi, G. Della Valle, M. Ornigotti, and P. Laporta

*Dipartimento di Fisica and Istituto di Fotonica e Nanotecnologie del CNR, Politecnico di Milano, Piazza L. da Vinci 32, I-20133 Milan, Italy*

(Received 20 July 2007; revised manuscript received 2 October 2007; published 1 November 2007)

We report on an experimental demonstration of light transfer in an engineered triple-well optical waveguide structure which provides a classic analog of coherent tunneling by adiabatic passage (CTAP) recently proposed for coherent transport *in space* of neutral atoms or electrons among tunneling-coupled optical traps or quantum wells [A. D. Greentree *et al.*, Phys. Rev. B **70**, 235317 (2004); K. Eckert *et al.*, Phys. Rev. A **70**, 023606 (2004)]. The direct visualization of CTAP wave-packet dynamics enabled by our simple optical system clearly shows that in the counterintuitive passage scheme light waves tunnel between the two outer wells without appreciable excitation of the middle well.

DOI: [10.1103/PhysRevB.76.201101](https://doi.org/10.1103/PhysRevB.76.201101)

PACS number(s): 42.82.Et, 05.60.Gg, 32.80.Qk

Similarities between quantum and classical phenomena are not uncommon in physics, albeit quantum and classical physics are based on different paradigms. Such analogies, which have been regarded as a mere curiosity until quite recently, have been fruitfully exploited in the past recent years in emerging research areas such as quantum computing, nanodevices, and new forms of light (see Ref. 1 and references therein). For instance, in its early developments the field of photonic crystals borrowed many ideas from solid-state physics.<sup>2</sup> Quantum-classical analogies in apparently unrelated fields have been also successfully exploited to mimic at a macroscopic level many quantum phenomena which are currently not of easy access in microscopic quantum systems. In particular, engineered photonic structures have proven to be a useful laboratory tool to investigate the optical analogs of a wide variety of quantum effects, including among others the optical analogs of Bloch oscillations,<sup>3-7</sup> Zener tunneling,<sup>6,8</sup> dynamic localization,<sup>9</sup> coherent enhancement and destruction of tunneling,<sup>10</sup> adiabatic stabilization of atoms in strong fields,<sup>11</sup> and Anderson localization.<sup>12</sup>

On the other hand, the ability of coherently manipulating the state evolution of a quantum system and of transferring a particle between positional quantum states in a controllable and reliable way is currently a subject of great relevance in quantum physics.<sup>13</sup> Recently, a robust scheme for coherent quantum transport *in space* of the wave function among tunneling-coupled quantum wells has been independently proposed for neutral atoms in optical traps<sup>14</sup> and for electrons in quantum dot systems<sup>15</sup> (see also Refs. 16 and 17). In such a scheme, which was referred to as “coherent tunneling adiabatic passage” (CTAP),<sup>15</sup> the tunneling interaction between adjacent quantum units is dynamically tuned by changing either the distance or the height of the neighboring potential wells following a counterintuitive scheme which is reminiscent of the celebrated stimulated Raman adiabatic passage (STIRAP) technique,<sup>18,19</sup> originally developed for transferring population between two long-lived atomic or molecular energy levels optically connected to a third auxiliary state. To date, however, no experimental demonstration of coherent transport in the space of a quantum particle by adiabatic passage has been reported.

In this Rapid Communication we show an experimental visualization of coherent transport of light waves by adia-

batic passage in an engineered optical waveguide system which provides the optical analog<sup>20-22</sup> of quantum CTAP in a dynamic triple-well potential. Our classic analog of CTAP enables a simple and direct visualization of the coherent wave-packet transport process, which is a rather unique possibility offered by optics.<sup>6</sup>

The optical structure we designed and manufactured consists of a set of three  $L=24$  mm long channel waveguides in the geometry shown in Fig. 1(a). Light trapped in one of the three waveguides may tunnel into the neighbor waveguide, the tunneling rate  $\Omega$  being controlled in our experiment by the waveguide distances. The left ( $L$ ) and right ( $R$ ) waveguides are far enough apart from each other that direct tunneling between them is fully negligible over the sample length. As the central ( $C$ ) waveguide is straight, the left and right waveguides are weakly curved, with opposite curvature of radius  $R$ , and longitudinally displaced from each other by a value  $\delta > 0$  so that their minimum distance  $a_{min}$  from the central waveguide is reached at different propagation lengths [see Fig. 1(a)]. The distances  $a_L(z)$  and  $a_R(z)$  of the left and right waveguides from the central one change along the paraxial propagation distance  $z$ , from the input ( $z=0$ ) to the output ( $z=L$ ) planes, according to the relations  $a_L(z) \approx a_{min} + (z-L/2)^2/(2R)$  and  $a_R(z) \approx a_{min} + (z-L/2 - \delta)^2/(2R)$ . With a proper engineering of the coupling rate between adjacent waveguides, the designed coupling geometry is suited to mimic CTAP. The quantum-optical analogy is at best captured starting from the Schrödinger-like paraxial wave equa-

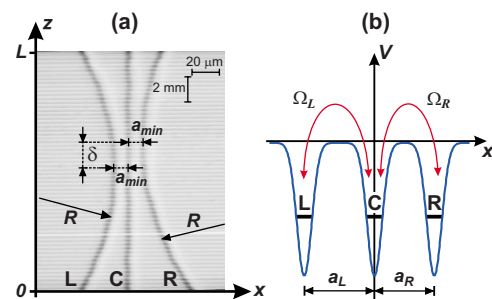


FIG. 1. (Color online) (a) Microscope image (top view) of the manufactured three-waveguide structure. (b) Schematic of light transfer in a triple-well system with controlled hopping rates.

tion describing monochromatic light propagation at wavelength  $\lambda$  along the paraxial direction  $z$  of the optical structure (see, for instance, Ref. 10):

$$i\lambda \frac{\partial \psi}{\partial z} = -\frac{\lambda^2}{2n_s} \nabla_{x,y}^2 \psi + V(x,y,z)\psi, \quad (1)$$

where  $\lambda \equiv \lambda/(2\pi)$  is the reduced wavelength,  $V(x,y,z) = [n_s^2 - n^2(x,y,z)]/(2n_s) \approx n_s - n(x,y,z)$  is the  $z$ -dependent triple-well potential,  $n(x,y,z)$  is the refractive index profile of the three-waveguide system at plane  $z$ ,  $n_s$  is the reference (substrate) refractive index, and  $|\psi|^2$  is proportional to the local light intensity. Indicating by  $c_L$ ,  $c_C$ , and  $c_R$  the amplitudes of the fundamental modes in the three waveguides, a coupled-mode equation analysis of Eq. (1) leads to the following STIRAP-like equations describing optical tunneling among the three waveguides:<sup>21,22</sup>

$$i \frac{dc_L}{dz} = -\Omega_L(z)c_C, \quad (2)$$

$$i \frac{dc_C}{dz} = -\Omega_L(z)c_L - \Omega_R(z)c_R, \quad (3)$$

$$i \frac{dc_R}{dz} = -\Omega_R(z)c_C, \quad (4)$$

where  $\Omega_L(z) = \Omega(a_L(z))$ ,  $\Omega_R(z) = \Omega(a_R(z)) = \Omega_L(z - \delta)$ , and  $\Omega(a)$  is the tunneling rate between two adjacent waveguides placed at distance  $a$ . Note that the temporal variable of the analog atomic STIRAP process<sup>18</sup> is here played by the spatial propagation distance  $z$ , whereas the Rabi frequencies of pump and Stokes pulses correspond to the  $z$ -dependent tunneling rates  $\Omega_L(z)$  and  $\Omega_R(z)$  [see Fig. 1(b)]. Note also that, as, for  $\delta > 0$ ,  $\Omega_L(z)$  precedes  $\Omega_R(z) = \Omega_L(z - \delta)$ , the counterintuitive (intuitive) pulse sequence of atomic STIRAP is simulated here by exciting the right (left) waveguide at  $z=0$ . Light transfer from the right to the left waveguides leaping over the central one is related to the existence of a dark state for Eqs. (2)–(4), given by  $(c_L, c_C, c_R) = (\Omega_R/\sqrt{\Omega_R^2 + \Omega_L^2}, 0, -\Omega_L/\sqrt{\Omega_R^2 + \Omega_L^2})$ . Light transfer is simply achieved by adiabatic change of the tunneling rates so that at the initial and final propagation planes the dark state corresponds to light trapped in the right and left waveguides, respectively.

In our experiment, the waveguides were fabricated by the Ag-Na ion exchange technique and applying a titanium mask onto an Er:Yb-doped glass substrate (Schott IOG1).<sup>23</sup> The two-dimensional (2D) index profile  $n_w(x,y)$  of the single waveguide, shown in Fig. 2(a), was measured using a refracted-near-field profilometer (Rinck Elektronik) at a wavelength of 670 nm and fitted by the relation

$$n_w(x,y) \approx n_s + \Delta n [g(x-a/2) + g(x+a/2)]f(y), \quad (5)$$

where  $\Delta n \approx 0.0148$  is the peak index change,  $g(x) = \{\text{erf}[(x+w)/D_x] - \text{erf}[(x-w)/D_x]\} / [2\text{erf}(w/D_x)]$  and  $f(y) = [1 - \text{erf}(-y/D_y)]$  define the shape of the index profile parallel to the surface of the waveguide ( $x$  direction) and perpendicular to the surface ( $y$  direction), respectively,  $2w \approx 5 \mu\text{m}$

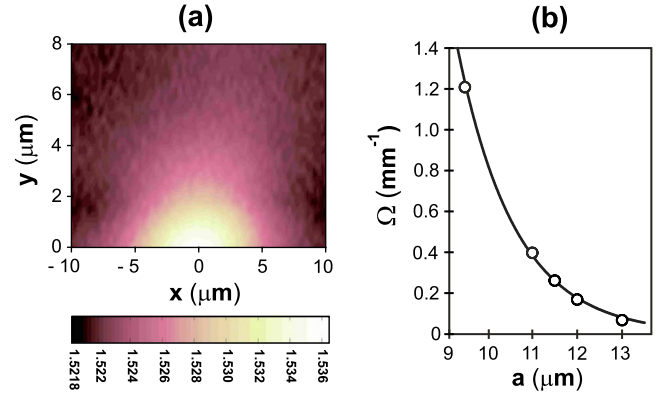


FIG. 2. (a) (Color online) Measured 2D refractive index profile  $n_w(x,y)$  of the Ag-Na diffused waveguide. (b) Measured tunneling rate  $\Omega$  between two waveguides versus waveguide distance  $a$  (circles). The solid curve is an exponential fit of the experimental data.

is the channel width, and  $D_x \approx 4.6 \mu\text{m}$  and  $D_y \approx 4.1 \mu\text{m}$  are the lateral and in-depth diffusion lengths. The waveguides have been excited at  $\lambda \approx 980 \text{ nm}$  wavelength using a single-frequency tunable laser diode fiber-coupled to the polished input facet of the sample. The probing light is partially absorbed by the  $\text{Yb}^{3+}$  ions (absorption length  $\sim 6 \text{ mm}$ ), yielding a bright green up-conversion luminescence arising from the radiative decay of higher-lying energy levels of  $\text{Er}^{3+}$  ions which is proportional to the local photon density of the probing radiation. The fluorescence was recorded from the top of the sample using a charge-coupled-device (CCD) camera connected to an optical microscope, providing a magnifica-

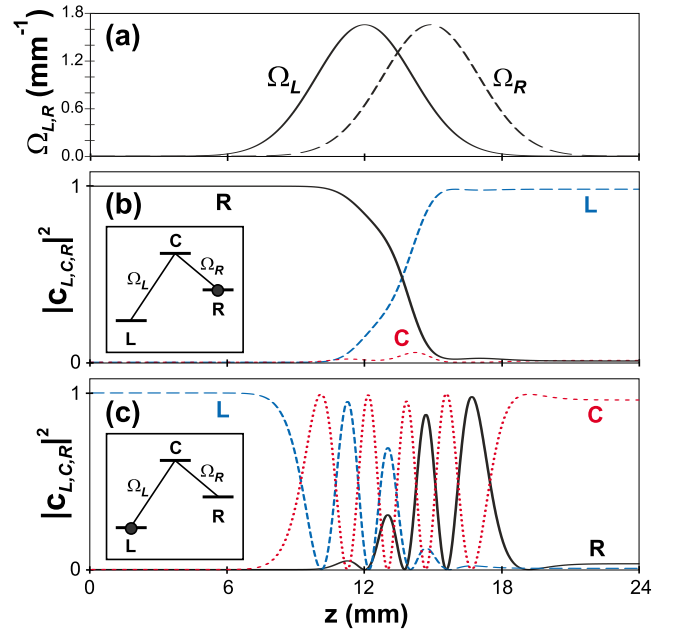


FIG. 3. (Color online) (a) Behavior of the tunneling rates  $\Omega_L$  and  $\Omega_R$  versus propagation distance  $z$  and behavior of fractional light power trapped in the three waveguides  $L$ ,  $C$ , and  $R$  versus  $z$  as obtained by coupled-mode equation analysis corresponding to (b) a counterintuitive pulse sequence (STIRAP) and (c) an intuitive pulse sequence. Parameter values are given in the text.

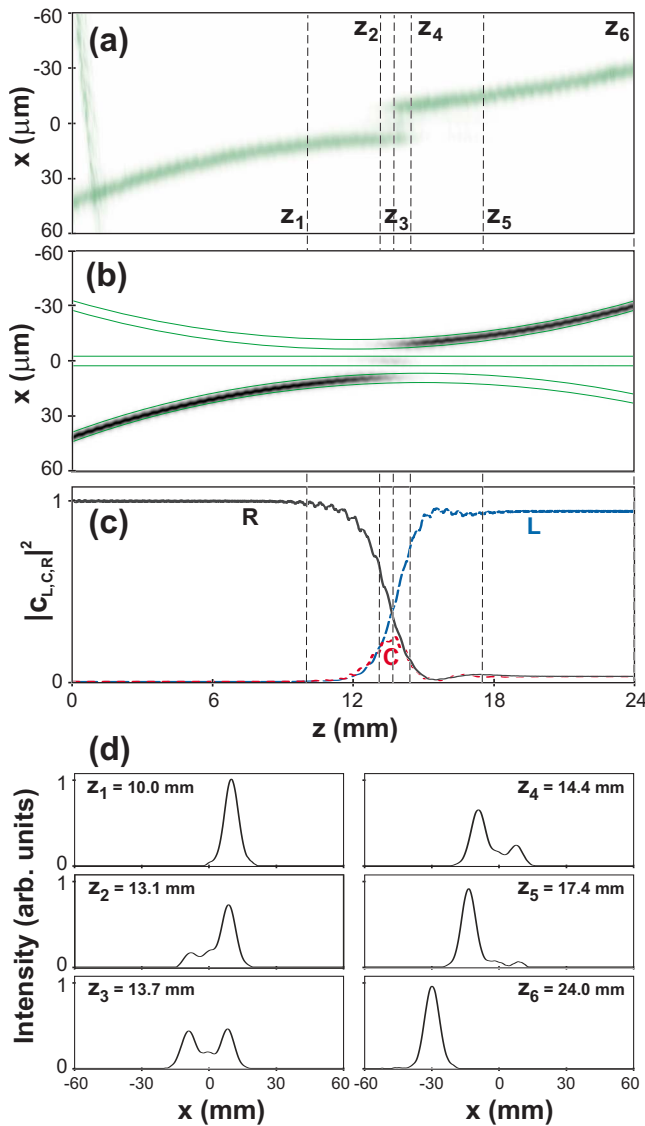


FIG. 4. (Color online) (a) Measured fluorescence pattern as recorded on the CCD camera (top view of the sample) corresponding to the input excitation of the right waveguide (CTAP). (b) Behavior of the light intensity distribution  $|\psi(x,0,z)|^2$  predicted by a numerical analysis of Eq. (1), and (c) corresponding fractional beam power trapped in the three waveguides versus propagation distance  $z$ . In (d) a few transverse cross sections of the measured fluorescence pattern are depicted at propagation distances corresponding to the vertical dashed lines in (a).

tion factor of  $\sim 12$ . The microscope was mounted onto a PC-controlled micropositioning system, and successive acquisitions of the fluorescence images along the paraxial propagation distance  $z$ , at steps of  $400 \mu\text{m}$ , allowed us to visualize step by step the flow of light along the three-waveguide system under different excitation conditions. The single-mode coupling fiber is mounted on a computer-controlled positioning system, which allows for precise control of the input beam launching conditions. Excitation of the fundamental mode of either the left or right waveguide with good mode matching is simply accomplished by scanning the fiber transversely along the input facet of the sample.

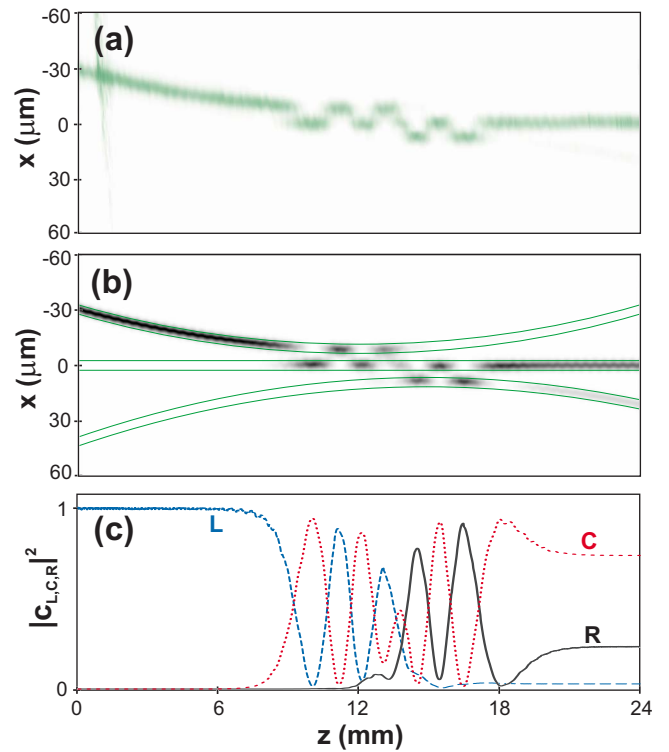


FIG. 5. (Color online) Same as Fig. 4, but for excitation of the left waveguide at the input plane (intuitive pulse sequence).

The parameters  $R$ ,  $a_{min}$ , and  $\delta$  which determine the behavior of tunneling rates  $\Omega_{L,R}(z)$  have been designed in order to fulfill the adiabaticity criterion requested for the observation of STIRAP.<sup>18</sup> To this aim, we preliminarily performed a set of accurate experimental measurements to determine the tunneling rate  $\Omega(a)$  of two adjacent waveguides versus their distance  $a$ . This was accomplished by manufacturing five two-waveguide straight couplers, with different waveguide interspacing ( $a=9.5 \mu\text{m}$ ,  $a=11.0 \mu\text{m}$ ,  $a=11.5 \mu\text{m}$ ,  $a=12.0 \mu\text{m}$ , and  $a=13.0 \mu\text{m}$ ) and by measuring the spatial period of the light tunneling pattern observed on the top of the sample. The experimental results, shown in Fig. 2(b), indicate that the tunneling rate dependence versus distance  $a$  may be well fitted by the exponential curve  $\Omega(a) = \Omega_0 \exp[-\gamma(a-a_0)]$  with  $\Omega_0 \approx 1.789 \text{ mm}^{-1}$  and  $\gamma \approx 0.7759 \mu\text{m}^{-1}$ , at least for distances  $a \geq a_0 = 9 \mu\text{m}$ . Using such a relation, a possible combination of parameter values for  $a_{min}$ ,  $R$ , and  $\delta$  that ensure adiabaticity of the STIRAP process and optimal overlap between pump and probe pulses was determined from a numerical analysis of the coupled-mode equations (2)–(4). As an example, Fig. 3 shows the numerically computed behavior of the normalized mode power  $|c_L|^2$ ,  $|c_C|^2$ , and  $|c_R|^2$  trapped in the three waveguides versus propagation distance  $z$  for an initial excitation of the right waveguide, corresponding to a counterintuitive pulse sequence (STIRAP) [Fig. 3(b)], and for the excitation of the left waveguide, corresponding to an intuitive pulse sequence [Fig. 3(c)]. The parameter values used in the simulations, which correspond to the manufactured structure shown in Fig. 1(a), are  $R=3.445 \text{ m}$ ,  $a_{min}=9.1 \mu\text{m}$ , and  $\delta=2.9 \text{ mm}$ . Figures 4(a) and 5(a) show the measured fluorescence pat-

terns as obtained by excitation of the right (Fig. 4) and left (Fig. 5) waveguides. In Fig. 4, the transverse cross-section profiles of the measured fluorescence pattern at a few propagation distances are also depicted. In Figs. 4(b) and 5(b), we plotted the corresponding images of light pattern evolution  $|\psi(x, 0, z)|^2$  as predicted by direct numerical simulations of the paraxial wave equation (1) using a standard beam propagation software (BEAMPROP 5.0) and assuming  $n(x, y, z) \approx n_w(x, y) + n_w(x - a_R(z), y) + n_w(x + a_L(z), y)$  for the index profile. The fractional light power trapped in the three waveguides versus propagation distance  $z$ , as obtained by the beam propagation analysis, is also reported. Note that the experimental results are very well reproduced by the numerical simulations. In particular, in the counterintuitive tunneling scheme of Fig. 4 the phenomenon of CTAP is clearly demonstrated since a high-efficiency transfer of light from the right to the left waveguides is observed with small excitation of the central waveguide. Conversely, in the intuitive tunneling sequence of Fig. 5 a complex tunneling scenario

among the three waveguides, with most of the power finally left in the central waveguide, is observed and well reproduced by the numerical analysis. It should be finally noted that the fraction of light power transiently trapped in the central waveguide and visible in Fig. 4, though relatively small, could be further reduced using longer waveguides. In fact, the limit to the transient power in the middle waveguide in the CTAP protocol as visible also from Fig. 3(b) is ultimately set by the adiabaticity of the process (see Refs. 18 and 19).

In conclusion, we reported on a classic wave optics analog of coherent transport of quantum particles by adiabatic passage, recently proposed as a robust mean to transfer neutral atoms or electrons in space.<sup>14,15</sup> Our optical analogy enabled a direct visualization of the tunneling transfer process and clearly demonstrated that in the scheme mimicking the counterintuitive pulse sequence of atomic STIRAP light waves are transferred to the outer wells with small excitation of the central one.

- 
- <sup>1</sup>D. Dragoman and M. Dragoman, *Quantum-Classical Analogies* (Springer, Berlin, 2004).
- <sup>2</sup>J. D. Joannopoulos, P. R. Villeneuve, and S. Fan, *Nature* (London) **386**, 143 (1997).
- <sup>3</sup>R. Morandotti, U. Peschel, J. S. Aitchison, H. S. Eisenberg, and Y. Silberberg, *Phys. Rev. Lett.* **83**, 4756 (1999); T. Pertsch, P. Dannberg, W. Elflein, A. Bräuer, and F. Lederer, *ibid.* **83**, 4752 (1999).
- <sup>4</sup>R. Sapienza, P. Costantino, D. Wiersma, M. Ghulinyan, C. J. Oton, and L. Pavesi, *Phys. Rev. Lett.* **91**, 263902 (2003).
- <sup>5</sup>D. N. Christodoulides, F. Lederer, and Y. Silberberg, *Nature* (London) **424**, 817 (2003).
- <sup>6</sup>H. Trompeter, T. Pertsch, F. Lederer, D. Michaelis, U. Streppel, A. Bräuer, and U. Peschel, *Phys. Rev. Lett.* **96**, 023901 (2006).
- <sup>7</sup>H. Trompeter, W. Krolikowski, D. N. Neshev, A. S. Desyatnikov, A. A. Sukhorukov, Y. S. Kivshar, T. Pertsch, U. Peschel, and F. Lederer, *Phys. Rev. Lett.* **96**, 053903 (2006).
- <sup>8</sup>M. Ghulinyan, C. J. Oton, Z. Gaburro, L. Pavesi, C. Toninelli, and D. S. Wiersma, *Phys. Rev. Lett.* **94**, 127401 (2005).
- <sup>9</sup>S. Longhi, M. Marangoni, M. Lobino, R. Ramponi, P. Laporta, E. Cianci, and V. Foglietti, *Phys. Rev. Lett.* **96**, 243901 (2006); R. Iyer, J. S. Aitchison, J. Wan, M. M. Dignam, and C. M. de Sterke, *Opt. Express* **15**, 3212 (2007).
- <sup>10</sup>I. Vorobeichik, E. Narevicius, G. Rosenblum, M. Orenstein, and N. Moiseyev, *Phys. Rev. Lett.* **90**, 176806 (2003); G. Della Valle, M. Ornigotti, E. Cianci, V. Foglietti, P. Laporta, and S. Longhi, *ibid.* **98**, 263601 (2007).
- <sup>11</sup>S. Longhi, M. Marangoni, D. Janner, R. Ramponi, P. Laporta, E. Cianci, and V. Foglietti, *Phys. Rev. Lett.* **94**, 073002 (2005).
- <sup>12</sup>T. Schwartz, G. Bartal, S. Fishman, and M. Segev, *Nature* (London) **446**, 55 (2007).
- <sup>13</sup>P. Kral, I. Thanopoulos, and M. Shapiro, *Rev. Mod. Phys.* **79**, 53 (2007).
- <sup>14</sup>K. Eckert, M. Lewenstein, R. Corbalan, G. Birkl, W. Ertmer, and J. Mompart, *Phys. Rev. A* **70**, 023606 (2004).
- <sup>15</sup>A. D. Greentree, J. H. Cole, A. R. Hamilton, and L. C. L. Hollenberg, *Phys. Rev. B* **70**, 235317 (2004).
- <sup>16</sup>K. Eckert, J. Mompart, R. Corbalan, M. Lewenstein, and G. Birkl, *Opt. Commun.* **264**, 264 (2006); E. M. Graefe, H. J. Korsch, and D. Witthaut, *Phys. Rev. A* **73**, 013617 (2006).
- <sup>17</sup>J. Siewert and T. Brandes, *Adv. Solid State Phys.* **44**, 181 (2004); L. C. L. Hollenberg, A. D. Greentree, A. G. Fowler, and C. J. Wellard, *Phys. Rev. B* **74**, 045311 (2006); U. Hohenester, J. Fabian, and F. Troiani, *Opt. Commun.* **264**, 426 (2006).
- <sup>18</sup>K. Bergmann, H. Theuer, and B. W. Shore, *Rev. Mod. Phys.* **70**, 1003 (1998).
- <sup>19</sup>N. Y. Vitanov, T. Halfmann, B. W. Shore, and K. Bergmann, *Annu. Rev. Phys. Chem.* **52**, 753 (2001).
- <sup>20</sup>A. M. Kenis, I. Vorobeichik, M. Orenstein, and N. Moiseyev, *IEEE J. Quantum Electron.* **37**, 1321 (2001).
- <sup>21</sup>S. Longhi, *Phys. Rev. E* **73**, 026607 (2006); *Phys. Lett. A* **359**, 166 (2006).
- <sup>22</sup>E. Paspalakis, *Opt. Commun.* **258**, 31 (2006).
- <sup>23</sup>G. Della Valle, S. Taccheo, P. Laporta, G. Sorbello, E. Cianci, and V. Foglietti, *Electron. Lett.* **42**, 632 (2006).